## WISP Processing

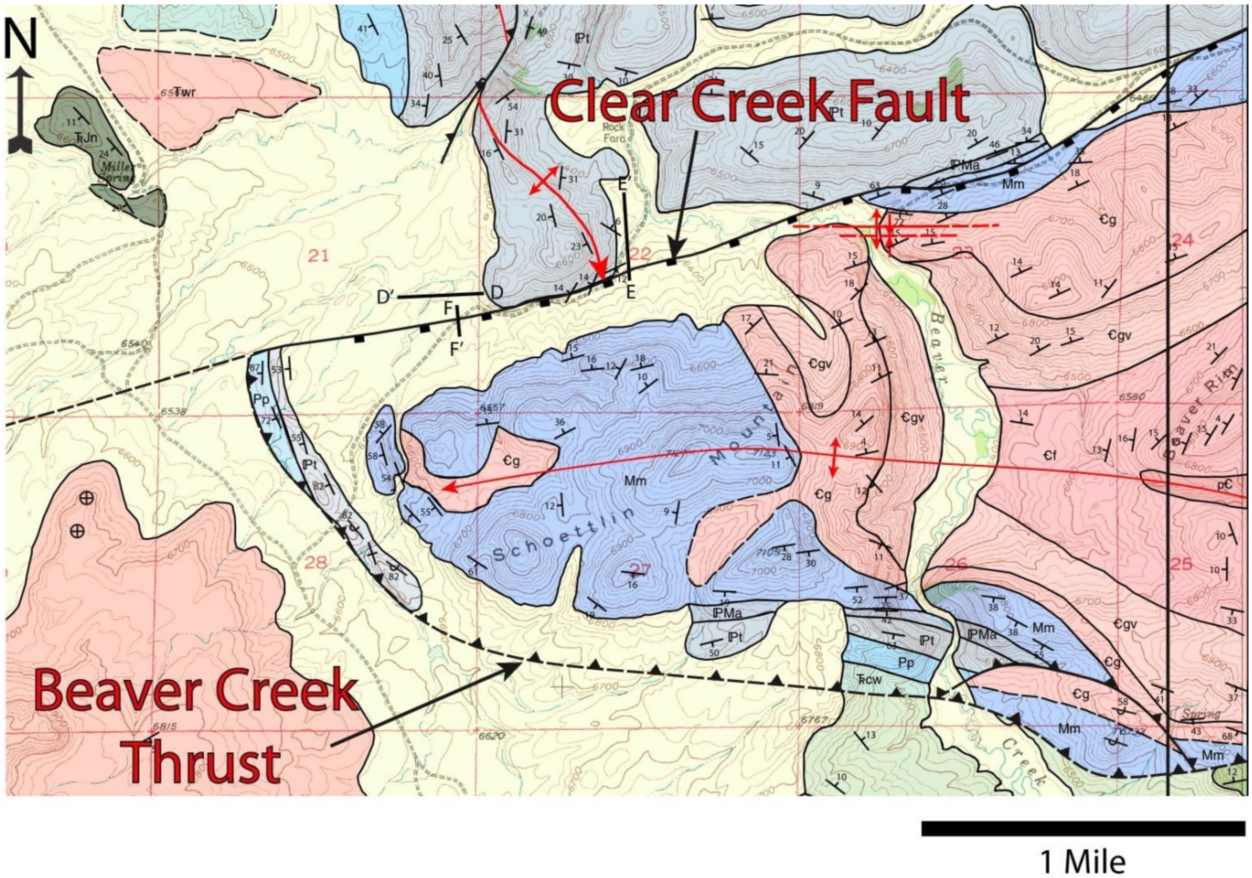


Figure 1: Enlarged map view of the E-W trending Clear Creek Fault, Beaver Creek Thrust, and Schoettlin Mountain Anticline (from Alward, 2010). See the map legend for Plate 1 for a key to the rock unit designations and map symbols used.

## Introduction

Previous studies of en echelon basin margin fold sequences have primarily used a combination of surface mapping, fracture analysis, well log analysis, and geologic cross sections to analyze the interchanges between domes (Ambercrombie, 1989; Meinen, 1993; Willis and Groshong, 1993; Gay, 1999; Brocka, 2007; and Clements, 2008). The use of seismic imaging techniques to constrain faults related to folding or the formation of the interchanges has been very limited (Cercone, 1989; Skeen and Ray, 1983; and Alward, 2010). This experiment was specifically designed to use 2D seismic reflection and refraction techniques to help resolve this problem. Our objectives were

1. Image the Carr Reservoir Fault and constrain its geometry at depth. Evidence suggests that this fault was affected by multiple periods of Laramide stresses, including late stage N-S compression.
2. Ascertain the extent to which N-S compression contributed to the formation of the south Derby Dome – north Sheep Mountain Anticline interchange, as well as in surrounding areas.

The seismic reflection and refraction data were collected in the field along two profiles: seismic line 1 (D-D'), seismic line 2 (E-E'). The equipment used in this experiment include: 104 Geometrics receivers (geophones), three 24-channel and two 16-channel Geometrics geode data acquisition boxes, an 8 gauge Betsy Seisgun source, and all associated cabling. A fixed spread geometry was used for the first seismic profile (D-D') with a total spread length of 274 meters. The second seismic profile (E-E') used a modified rolling spread geometry, in which shots were performed up to the first geophone, after which a designated section of the line was moved to the end of the profile. Shots were executed in both the forward and reverse directions. E-E' had a total spread length of 484 meters. Total shots for seismic line 1 (D-D') and 2 (E-E') were 35 and 53 respectively. A complete description of line design and parameters can be found in Tables 1 and 2.

Table 1: Seismic Line 1- Fixed

| | |
|---|---|
| Source Type: | Betsy Gun – 8 ga. |
| Source Depth: | ~ 1.5' |
| Receiver Type: | 104 geophones |

| | |
|---|---|
| Data Recording System: | 3 – 24 channel Geodes and 2- 16 channel Geodes |
| Recording Time: | 1 s |
| Sampling Interval: | 0.25 ms |
| Source Spacing: | 8 meters |
| Receiver Spacing: | 2 meters |
| Total Spread Length: | 272 meters |
| Total Shots: | 35 |
| Fold: | 12 |

## Procedure

This experiment used a fixed spread design. This means that shots were performed throughout the entire spread and the geophones were not moved during the experiment. 4 shots were performed before the first geophone and 5 shots were performed after the last geophone.

Table 2: Seismic Line 2- Modified Rolling

| | |
|---|---|
| Source Type: | Betsy Gun – 8 ga. |
| Source Depth: | ~ 1.5’ |
| Receiver Type: | 104 geophones |
| Data Recording System: | 3 – 24 channel Geodes and 2- 16 channel Geodes |
| Recording Time: | 1 s |
| Sampling Interval: | 0.25 ms |
| Source Spacing: | 6 meters |
| Receiver Spacing: | 2 meters |
| Total Spread Length: | 484 meters |
| Total Shots: | 53 |

Shots were performed up to the first geophone. Upon reaching the first geophone a designated section of the line was moved to the end of the spread.

Procedure

1. 5 shots performed
2. 48 m of the line moved to the end of the spread
3. 8 shots performed
4. 48 m of the line moved to the end of the spread
5. 8 shots performed
6. 48 m of the line moved to the end of the spread
7. 8 shots performed
8. 32 m of the line moved to the end of the spread
9. Final 5 shots performed in the forward direction
10. The profile is adjusted for the reverse shots the 6 shots performed
11. 48 m of the line moved to the end of the spread
12. 8 shots performed
13. 32 m of the line moved to the end of the spread
14. Final 5 shots performed in the reverse direction

## Methodology

### *Field Methods*

To begin each experiment, the length of the profile selected was measured and flagged. Seismic line 1 (D-D') and 2 (E-E') were shot separately using a fixed and modified rolling spread respectively. For both lines, a 0.5m hole was dug and filled with water at every predetermined source location. Each source hole was filled with water to increase coupling and signal to noise ratio. Each completed shot was recorded and compiled using Geometrics software on a field laptop computer.

### *Data Processing*

### Seismic Reflection Processing

All seismic reflection data were processed and analyzed using Geo2x's Visual SUNT_20 pro. To begin the process, all reflection data were converted from SEG2 to Seismic Unix (SU) format. After the conversion, all linear noise associated with source airwave and ground roll (portions of the traces that are not reflections) were minimized by applying bandpass filters and then manually deleted from each shot gather. Next, the specific geometry of each line was applied. This consisted of inputting the number of receivers, source and receiver spacing, and source and receiver location for each profile. Following the application of the geometry, each profile was sorted into common depth point (CDP) gathers. A constant velocity scan-constant velocity stacking panel command was applied to the sorted CDP gathers to determine velocities used to apply a normal moveout correction (NMO). To complete this step, the range of stacking velocities used must be specified, beginning with the absolute minimum possible velocity (~500 m/s) extending to the highest possible velocity (~3500m/s). Data sets were then stacked using the estimated NMO velocities. The final profile was altered/improved by varying the stacking velocities and varying the velocities laterally.

## Seismic Refraction Tomography

Refraction tomography processing and analysis was conducted using SeisImager programs PickWin95 and Plotrefa. Processing began by evaluating the variations in P-wave speed. This was done by picking the first P-wave arrivals for every 3$^{rd}$ shot file using PickWin95. These picks were then imported into Plotrefa. Next, best fit velocity lines and inflection points were picked for each layer present. Following the first motion picking, a time-term analysis was implemented to computationally account for topographic and interface variations. Finally, a refraction tomography technique was applied to map lateral variations in velocity. To complete this step, an initial model must first be generated. The generated initial time-term model was then used for the refraction tomography by performing a tomographic inversion analysis to produce a final tomogram. For the final tomogram, a five-layer analysis was preformed, which included other parameters such as: number of iterations, number of nodes, amount and weight of horizontal and vertical smoothing, and the minimum and maximum velocity of the initial time term model.

## Results & Interpretations

The following describes the final images from the 2D seismic reflection and refraction processing as well as a summary of the interpretations made from each profile by the author.

### *Seismic Reflection*

#### Seismic Profile 1 (D-D')

The final processed image for seismic profile 1 (Fig. 2) is a 12-fold resolution image. This profile has a 4.4 times horizontal exaggeration at 2.4 km/s (100ms = ~ 120m). The deepest reflections imaged on this east-west oriented line are roughly 400ms or 480 m deep. The primary interpretation for this reflection profile is correlated with the results of geologic mapping. The major feature observed on this reflection profile is the Carr Reservoir Fault. The top reflections display minimal offset and are interpreted to represent Quaternary fill deposited on/over the fault scarp. Deeper reflections (~125-150 ms) display larger offsets along the fault (~80 m or ~260 ft of throw), which is more indicative of the Carr Reservoir Fault (Plate 4). The location of the fault correlates well with the observed surface geology.

## Seismic Profile 2 (E-E')

The final processed image for seismic profile 2 (Fig. 3) is a 17-fold resolution image. This profile trends NE-SW and crosses the Carr Reservoir Fault. Profile E-E' has a 2.3 times horizontal exaggeration at 2.8 km/s (100ms = ~ 140m). The deepest reflections imaged on this profile are roughly 450-500 m deep. Areas that display a loss of strong reflectors (~140m depth) are interpreted to represent a distinct lithologic change from the Alcova Limestone to the less reflective siltstone and mudstone of the Red Peak Formation. The odd shape of the profile is due to the muting style and the unique geometric design of the line. This profile was shot using a modified rolling spread and was processed using shots that progressed from NE-SW and also SW-NE. The primary

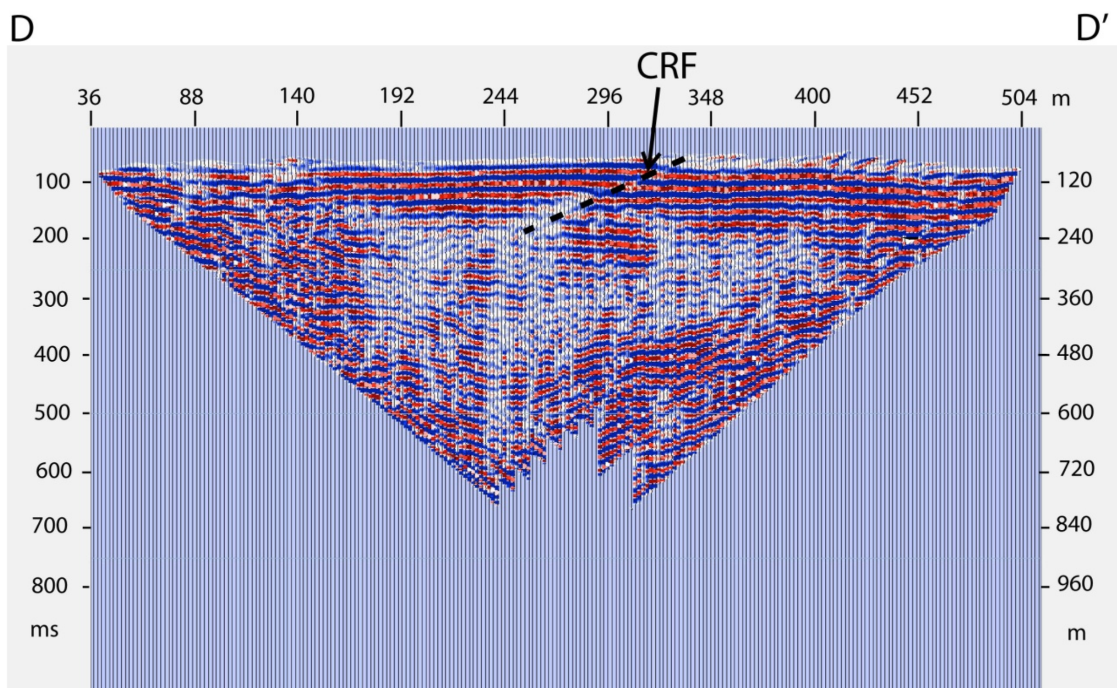


Figure 2: Seismic reflection profile 1 (D-D') displayed in TWTT (left vertical scale) and depth (right vertical scale). Note the location of the Carr Reservoir Fault (CRF).

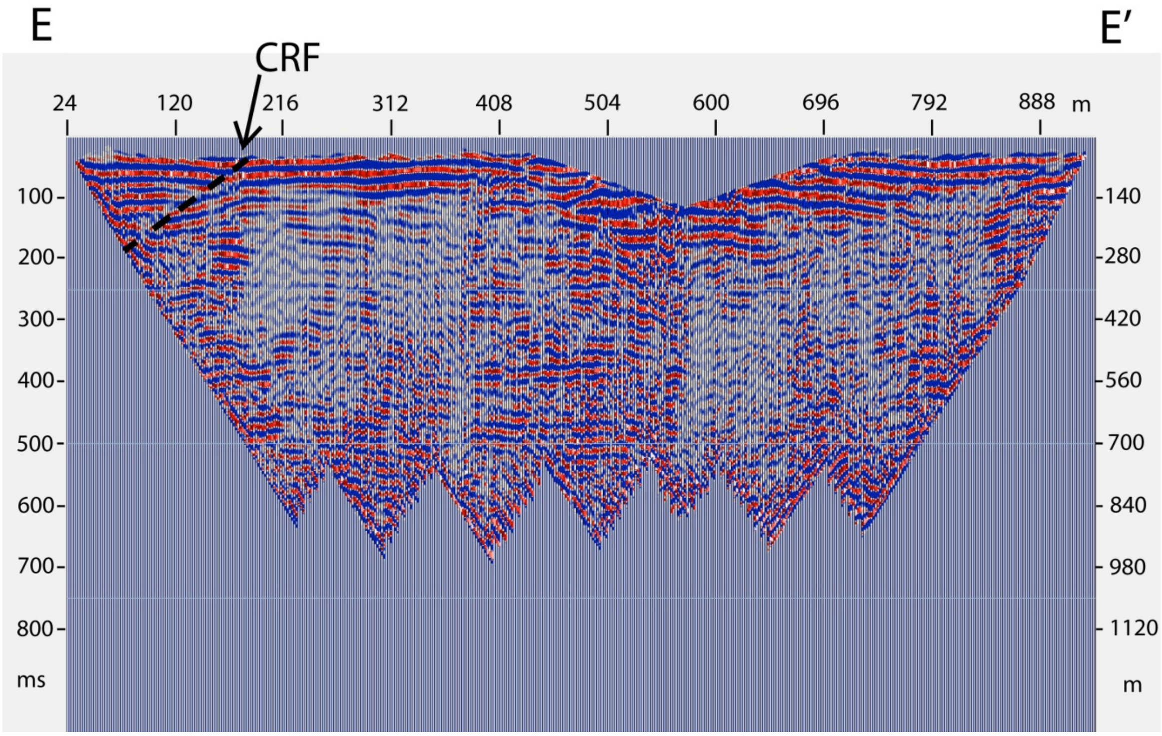


Figure 3: Seismic reflection profile 2 (E-E') displayed in TWTT (left vertical scale) and depth (right vertical scale) displaying the Carr Reservoir Fault (CRF).

feature observed on this reflection profile is again the Carr Reservoir Fault located near the northeastern most portion of the profile. Reflections between 75-150 ms (~105-210 m)display approximately 85m or 280 ft of throw along the fault. The location and observed offset of this fault (Carr Reservoir Fault) correlate very well with mapped surface geology.

### *Seismic Refraction*

### Seismic Profile 1 (D-D')

The two figures presented for this section are: 1) the time inversion model used to generate the initial model used in the tomographic inversion process (Fig. 3), and 2) the final tomogram (Fig. 4). The final tomogram was created using a flat surface model, meaning the lateral and vertical velocity variations displayed across D-D' are not a function of topography.

The average error for this tomogram is 2.08 ms. Both the time inversion model and the final tomogram display a deep region of low velocity which is consistent with the presence of a fault zone. This area of low velocity correlates well with the location of the Carr Reservoir Fault observed from surface geology.

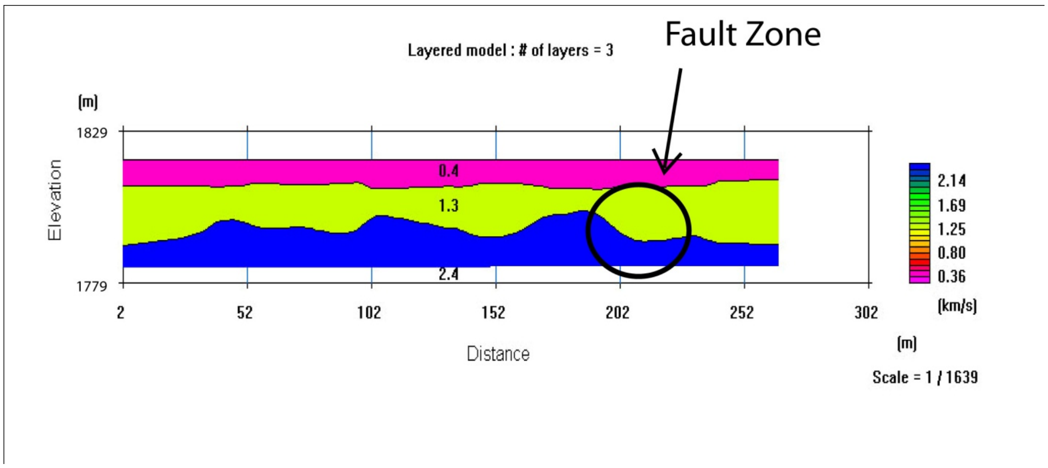


Figure 4: Time term inversion model used to create the final tomogram. Note the location of the interpreted fault zone.

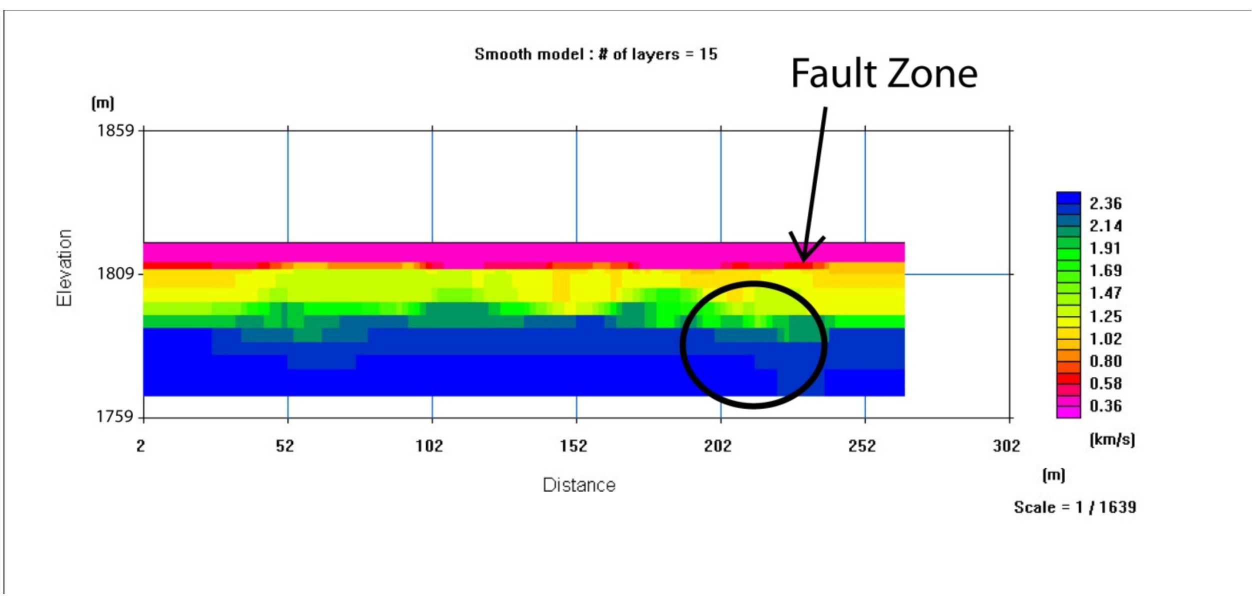


Fault 5: Final processed tomogram. Note the indicated zone of low velocity which is indicative of a fault zone.

## Discussion

### *Data Acquisition Challenges*

The main challenges in the acquisition of data were the rugged terrain in the Wind River Basin and access to desired areas of study. When selecting specific areas to perform the seismic study two questions must be addressed: 1) how difficult is the study area to access?, and 2) will the experiment design (geometry/location/orientation) provide the best possible results? The first area selected (labeled Seismic Profile 1on the map) was difficult to reach due to rough terrain and limited road access. Because of access problems and limited area to perform the experiment, this line was shot using a fixed spread with a shorter profile length (<300m). The second seismic profile study area had much easier access and a larger region to perform the experiment. Because of these factors the second profile was shot using a modified rolling spread and longer profile length (~500m).

### *Seismic Reflection Processing Challenges*

During the processing of the seismic reflection data certain, challenges arose. To begin, the seismic data contained significant source-related noise that must be minimized and later deleted. Bandpass filters were applied to deal with low frequency ground roll (40Hz-100Hz) in order to minimize ground roll and maximize reflections. The remaining ground roll had to be eliminated and was manually deleted from each shotgather. This deletion process resulted in the loss of large portions of signal, including reflection signal covered by the ground roll. This muting process played a role in the final shape and resolution of each reflection profile. The next challenge that arose was the application of the geometry of each profile. This was especially true for seismic profile 2 (E-E'), which consisted of a modified rolling spread shot in both the forward and reverse directions. This complicated geometry required careful attention to complete.

## Conclusions

The following conclusions were derived from the 2D seismic reflection and refraction experiment:

- The seismic reflection portion of the experiment successfully imaged (Fig. 2 and 3) the Carr Reservoir Fault, and confirmed that the fault is a high angle, NE-side-up reverse fault, that displays approximately 280 ft of vertical throw, which is consistent with the initial field mapping observations.
- The seismic reflection experiment design was successful in imaging shallow structures to an approximate depth of 450 meters.
- Both fixed and rolling profile designs produced useful results.
- The seismic refraction portion of the experiment displays an area of low velocity, which is consistent with the presence of a fault zone. This correlates well with the mapped surface location of the Carr Reservoir fault.

The extent that N-S compression played in the formation of the interchange between south Derby Dome and north Sheep Mountain Anticline could not be determine from the seismic reflection and refraction profiles alone